Peer-reviewed version available at Remote Sens. 2018, 10, 386; doi:10.3390/rs10030386

Article

The Role of NWP Filter for the Satellite Based Detection of Cumulonimbus Clouds

Richard Müller [1]* , Stephane Haussler [1] and Matthias Jerg [1],

[1] German Weather Service, Frankfurter Str 135, 63067 Offenbach, Germany
* Correspondence: Richard.Mueller@dwd.de; Tel.: +49-(0)69-8062-4922

Abstract: The study investigates the role of NWP filtering for the remote sensing of Cumulonimbus Clouds (Cbs) by implementation of 14 different experiments, covering Central Europe. These experiments compiles different stability filter settings as well as the use of different channels for the InfraRed (IR) brightness temperatures. As stability filter parameters from Numerical Weather Prediction (NWP) are used. The brightness temperature information results from the IR SEVIRI instrument on-board of Meteosat Second Generation satellite and enables the detection of very cold and high clouds close to the tropopause. The satellite only approaches (no NWP filtering) result in the detection of Cbs with a relative high probability of detection, but unfortunately combined with a large False Alarm Rate (FAR), leading to a Critical Success Index (CSI) below 60 %. The false alarms results from other types of very cold and high clouds. It is shown that the false alarms can be significantly decreased by application of an appropriate NWP stability filter, leading to the increase of CSI to about 70 % . A brief review and reflection of the literature clarifies that the this function of the NWP filter can not be replaced by MSG IR spectroscopy. Thus, NWP filtering is strongly recommended to increase the quality of satellite based Cb detection. Further, it has been shown that the well established convective available potential energy (CAPE) and the convection index (KO) works well as stability filter.

Keywords: cumulonimbus; thunderstorms; stability filter; aviation

1. Introduction

Cumulonimbus clouds (Cb) originate from rapid vertical updraft of humid and warm air enforced by constraint forces caused e.g. by mountains, heating or cold fronts. The fast cooling of the air with rising height leads to optically thick and very cold clouds, referred to as cumulonimbus clouds (Cbs), which are usually accompanied by lightning, heavy precipitation, hail, and turbulence. Early and reliable prediction of Cb clouds is therefore of great importance for weather forecasts and warnings, in particular for aviation, as Cb clouds (thunderstorms) constitute one of the most important natural risks for aircraft accidents. An accurate Cb detection and short term forecast enables cost-efficient planning and use of alternative routes, increasing flight safety.

Yet, the reliable simulation of convective cells and Cbs by means of numerical weather prediction is still a very difficult task. Thus, observational data plays a pivotal role for the accurate detection and short term forecast of Cbs. Over ocean and a vast number of countries, which are not well equipped with precipitation RADARs, satellites are in addition to global lightning ground based networks the only observational source for the detection of Cbs, e.g. [1]. As a result of the thermodynamics involved in the generation of Cbs they are optical thick and their tops are located close to the tropopause. Therefore, from a satellite perspective they are characterized by very cold brightness temperatures corresponding to high cloud top heights (CTH).

Thus, cloud top height is on option used as a straightforward method to provide information about the risk for cumulonimbus cloud occurrence as operated by e.g. NCAR ([2] and references therein). The cloud top height can be derived from the brightness temperature (BT) in the atmospheric window channel (InfraRed 10.6), which corresponds in good approximation to the temperature of the

Preprints (www.preprints.org) | NOT PEER-REVIEWED | Posted: 30 November 2017 doi:10.20944/preprints201711.0194.v1

Peer-reviewed version available at Remote Sens. 2018, 10, 386; doi:10.3390/rs10030386

cloud top for Cbs. A NWP based profile of the atmosphere can then be used to link the temperature to the height of the cloud top, see figure 1 for an example of an atmospheric profile. A more detailed discussion of methods for the estimation of CTH are presented in [3].

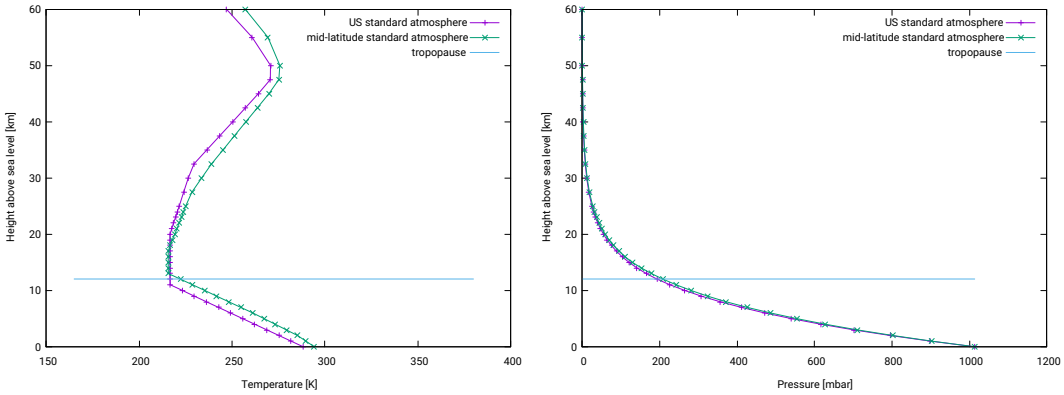

Figure 1. Left hand: The image shows the relation of the height above sea level and the temperature in the atmosphere for the US standard atmosphere and a standard atmosphere for mid-latitude summer. Diagrammed is also the height of the tropopause, which "separates" the troposphere from the stratosphere. Right hand: Relation between pressure and height for the same profile.

Another simple, but widely used method is that applied in the Global Convective Diagnostics approach [4] and [2]. The method uses the brightness temperature difference between the 6.7 μm the 11.6 μm infrared satellite channel, the former is also referred to as water vapour channel, cause of the large water vapour absorption bands. If the difference exceeds 1 degree it is assumed that the observed cloud is a cumulonimbus cloud. The physical background of this approach has been already discussed in 1997 by Schmetz et al. [5]. They investigated the potential of satellite observation for the monitoring of deep convection and overshooting tops. They found that the brightness temperature of the water vapor channel (5.7-7.1 μm) can be larger (warmer) than that of the IR window channel (10.5-12.5 μm). They demonstrated by radiative transfer modeling (RTM) that the larger brightness temperatures (BT) in the WV channel are due to stratospheric (tropopause) water vapor, which absorbs radiation from the cold cloud and subsequently emits radiation at higher temperature (warmer), as the temperature increases in the stratosphere, see figure 1. The effect is largest when the cloud top is at the tropopause temperature inversion. Optical thick high clouds cover the tropospheric water vapor and only the emission from the stratospheric water vapor contributes to the radiance observed by the satellite instrument. In contrast, for lower clouds the tropospheric water vapor above the clouds absorbs the radiation and the emitted radiation is colder than the absorbed. It is therefore obvious that the temperature difference increases with increasing cloud height.

The effect discussed by [5] occurs also if the difference of the two water vapor channels are used. The use of this combination is possible since the launch of Meteosat Second Generation satellites, which has the Spinning Enhanced Visible and InfraRed Image (SEVIRI) instrument on-board. This instrument is equipped with additional channels in the Infrared (IR). The normalized weighting function of the SEVIRI IR channels is diagrammed in Figure 2 for clear sky.

Note, that the water vapor channel at 6.2 μm receives significant contributions from the stratosphere, which are larger than the equivalent contributions of the WV channel at 7.3μm. Thus, the mechanism discussed by Schmetz et al [5] works also well for the difference of the water vapor channels.

A slightly different approach is used by the Nowcasting Satellite Application Facility NWC-SAF. This method is based upon an adaptive brightness temperature thresholds of infrared images [6]. Further, cloud classification methods have been developed which use texture information of the visible channels in addition to the brightness temperature thresholds to detect Cbs and other cloud types. The

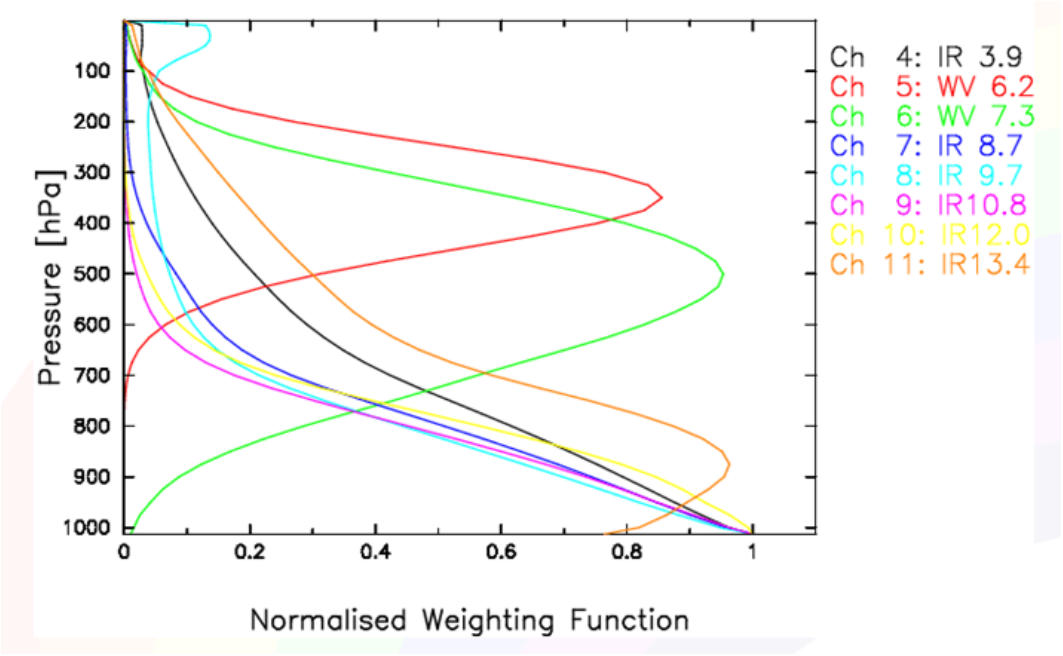

Figure 2. The image shows the normalized weighting function of MSG for clear sky , source Eumetrain

NRL Cloud Classification (CC) algorithm [7] is one example. It is used by the Oceanic Weather Product Development Team to assist in the accurate detection of deep convective clouds. Another example is the Berendes cloud mask [8]. However, in both methods visible channels are utilized and they are therefore not applicable during night. Thus, these approaches are not sufficient to provide a day and night service needed by aviation. Finally, there exists a commercially offered software package, which has been developed and validated by Zinner et. al [9] and references therein.

All these approaches use information from the IR region for the satellite based detection of Cbs. However, not only Cbs are optically thick and cold, but also other clouds, which can lead to serious false alarms. As briefly discussed in [2] these false alarms might be reduced by the implementation of an stability filer from NWP.

To the knowledge of the authors the above mentioned methods do either not apply an NWP filter (e.g. [6–9] or did not provide an extensive analysis and discussion of NWP filtering ([2,4]), e.g. by implementation of different experiments. Further, the role of NWP filtereing is not reflected in relation to IR spectroscopy. Thus, the central novel aspect of this work is the extensive discussion and analysis of NWP filtering for the quality of satellite based Cb detection, including a reflection of SEVIRI IR spectroscopy as alternative.

2. The method

The difference of the brightness temperature of the WV channels of the SEVIRI instrument on board of the Meteosat Second Generation satellite (MSG) is used as starting point of the study and in the majority of the experiments. This approach is based on the method discussed in [5] and more relevant to present times applied by e.g. [4] and [2]. However, in our method, the WV 7.3 channel is used instead of the atmospheric window channel for the calculation of the brightness temperature difference.

Further, in contrast to [2] a threshold of -1 *K* is applied in the first experiments. However, further experiments are performed with different thresholds. As the temperature signal of Cbs is not only apparent in the WV channels the performance of further channels combinations are investigated in the experiments as well.

For the stability filter the well established convective available potential energy (CAPE) is used [10]. CAPE is the amount of energy a parcel of air would have if lifted a certain distance vertically through the atmosphere. It is effectively the positive buoyancy of an air parcel.

As a supplementing filter to CAPE the Totals Total (TT) index has been used. It is defined as:

$$TT = T850 + Td850 - 2 * T500 \tag{1}$$

here T is the temperature, Td is the dew point temperature and the numbers provide the respective pressure level.

Further, the KO index defined in equation 2 have been applied in further experiments;

$$KO = \frac{1}{2} \cdot (\theta_{e_{700}} + \theta_{e_{500}} - \theta_{e_{1000}} - \theta_{e_{850}}) \qquad [K] \tag{2}$$

here θ_e is the pseudo potential temperature in Kelvin for the different pressure levels 1000, 850, 700 and 500 hPa.

The "stability" filters (CAPE and TT) for the first experiments (up to experiment 9) are taken from the comprehensive Earth-system model developed at ECMWF in co-operation with Météo-France. A detailed documentation of can be found at the ECMWF web-page, see [11] and concerning the convection part in [12]. The thresholds for the NWP stability filters (CAPE and TT) have been varied in the experiments (experiment 7,8), but for the reference experiment 1 they have been set to CAPE=60 and TOTALX=50. Within case studies (visual inspection) other "filter" variables provided by ECMWF have been investigated but have been excluded in the experiments due to their comparatively poor performance.

In order to investigate the sensitivity of the NWP filtering on the chosen NWP model CAPE has been also taken from from ICON [13] in experiment 10 and 11. Further, also KO has been generated by ICON.

In the experiments with the NWP filters a Cb can only occur if the stability filters exceeds the filter thresholds independent of the satellite signal. For the combination of CAPE and TOTALX it is an ore conjunction, thus a Cb is assigned if one of the two filter thresholds is exceeded. For experiments without NWP filter Cb occurs if the BT difference is higher than the BT threshold defined for the respective experiment. All experiments and settings are listed in table 1. Figure 3 illustrates the effect of the NWP filter on the satellite based Cb detection.

It is important to note that the stability indices are used to exclude Cb that are incorrectly detected by the satellite in stable and neutral atmospheres (e.g. cold fronts). Thus the thresholds applied for the stability filter are very low.

3. Results

3.1. Validation

Lightning data from a low frequency (VLF/LF) lightning detection network (LINET), discussed in [14] and [15], are used for validation. The measurement network provides cloud-to-ground lightning strokes (CG) and cloud lightning (IC). According to [14], the position accuracy reaches an average value of about 150 m, whereby false locations ('outliers') rarely occur.

Cloud lightning and cloud to ground lightning strokes are used for the validation if the amplitude is higher/lower than +/- 10 kA. A CB is defined as correctly detected if lightning occurs within a 10 minute time interval and an search region of $\pm$ 50km. If there is no lightning, then a false alarm is counted. Of course, also CB without strokes or artificial strokes are possible, but this is not accounted for. This means that the performance of the method might be slightly better than expressed in the skill scores. The search region (SR) of $\pm$ 50 km reflects the fact that larger Cbs are of most interest for aviation. Further, it accounts for the typical range of dislocations between lightning and the center of

Preprints (www.preprints.org) | NOT PEER-REVIEWED | Posted: 30 November 2017 doi:10.20944/preprints201711.0194.v1

Peer-reviewed version available at Remote Sens. 2018, 10, 386; doi:10.3390/rs10030386

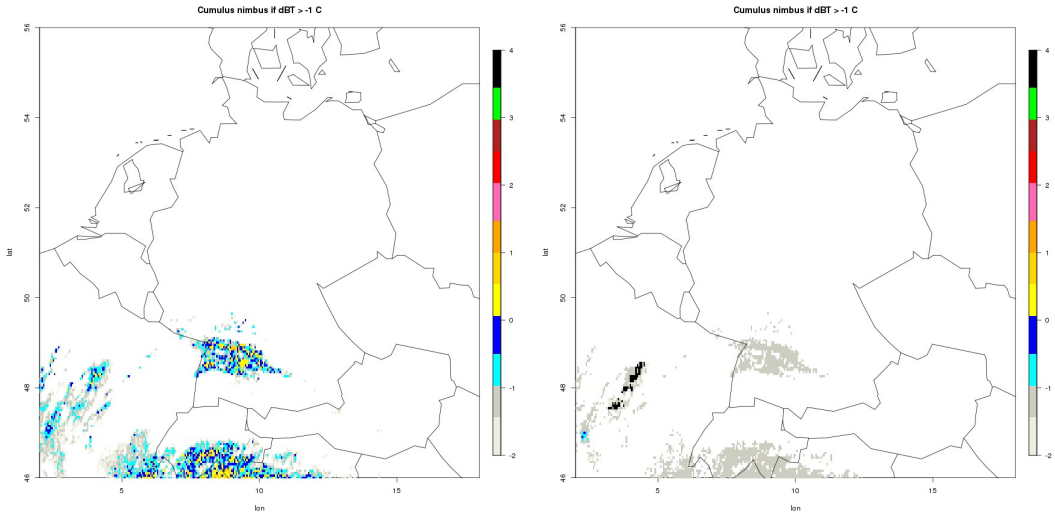

Figure 3. Example of NWP filtering for May 2016, 6 UTC. **left**. Satellite artificially detects Cb in the colored regions. Application of the NWP filter leads to a significant reduction of false alarms. However, the black regions are those where the NWP filtering fails and still false alarms occurs.

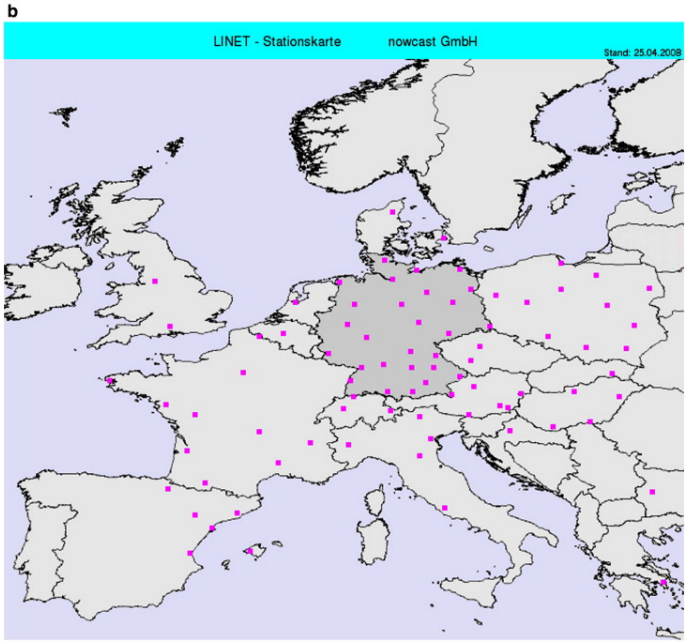

Figure 4. The LINET network , source LINET GMBH, taken from [14]

the Cb (approx. 15-20km), as well as for the geolocation error of the satellite (approx 5km), and for the security distance defined for flying round of a Cb. The study focuses on central Europe where the LINET network density is the highest, see Figure 4. The borders of the validation region are as follows: Latitude 45.5-56.5 N and Longitude 2.0-18.0 East.

The skill scores Probability Of Detection (POD), False Alarm Rate (FAR), Critical Success Index (CSI) are used to measure the performance of the different approaches. For completeness the quantities are defined below:

$$POD = CD/(CD + MD) \tag{3}$$

$$FAR = FD/(CD + FD) \tag{4}$$

$$CSI = CD/(CD + MD + FD) \tag{5}$$

Hereby, CD stands for Correct Detection of a Cb, MD stands for Missed Detection of a CB and FD stands for False Detection and CDN stands for Correct Detection of Nil. The validation is performed on a pixel basis. This means that each pixel is assigned with either CD, FD, MD or CDN. Missed detection is counted if lightning occurs but there is no Cb detected by the satellite within the search radius.

Experiments 1-11 have been performed performed for the period 10.05.16-09.06.16, for 6,9,12,15,18 UTC respectively. The experiments 12-14 dealing with KO and respective intercomparison experiments, needed to evaluate the KO skill scores, have been performed for June 2017. This has been necessary as KO is not archived for the 2016 period. Both periods are characterized by frequent occurrence of Cbs for different weather situations, seize and structure.

Two experiments have been performed using additionally the BT difference of the ozone channel (IR9.7) and the 8.7 channel (9.7-8.7). The IR9.7 channel is the ozone channel and has a clear sky emission peak in the stratosphere see figure 2. Thus, it can be assumed that clouds reaching the stratosphere (overshooting tops) show a pronounced signal if the ozone channel is used for the calculation of the BT difference as discussed e.g by [16]. Overshooting tops are a specific feature of Cbs. Thus, the use of the ozone channel might be useful to omit the NWP filter at a certain BT difference (height), which has been investigated in experiment 5 and 6. However, the physical basis is the same as discussed in [5], but with the ozone emission interacting with the cloud emission instead of water vapour/cloud interaction.

3.2. Results

Tables 1 shows the skill scores of the experiments in detail. Following the main results of the experiments are summarized.

The results show that applying a NWP filtering can be used to optimize the relation of POD and FAR and thus, to improve the critical success index. For the experiments with NWP filter a relative high POD in combination with a relative low FAR can be gained, leading to significant better CSI than without NWP filtering.

POD is slightly higher without NWP filtering, but FAR is strongly affected towards higher values, leading to a significant decrease of CSI. However, compared to the experiments without NWP filtering higher POD can be achieved, accompanied by better CSI and FAR, by application of the NWP filter and lowering of the BT difference threshold (Experiments 1-4). These results clearly demonstrates that the NWP filter does significantly increases the performance of the satellite based detection of Cbs. Thus, also for applications where a high POD is the primarily goal, and FAR and CSI are of second priority, the NWP filter is of significant benefit.

The additional usage of the O_3 channel does not lead to better skill scores compared to the reference (experiment 1). On the other hand, the one channel approach (experiment 9) leads to similar skill scores compared to the reference (experiment 1). The physical basis of these results is further discussed in section 4

Experiment 7 and 8 shows the effect of a slight variation of the NWP filter threshold on the skill scores. Finally in experiment 10 and 11 CAPE from ICON has been used instead of CAPE from ECMWF. The results show that the skill scores are not significantly affected by the NWP source for CAPE. Thus, the NWP filtering is not sensitive to the NWP model in our experiments.

Further experiments (12-14) for June2017 has been performed with KO from ICON as this stability filter has been recommended by the weather forecast department based on their daily practice. In order to evaluate the skill scores for KO intercomparison experiments for the same period has been performed with CAPE (as the skill scores are not independent on the chosen period). The investigated hours and the region are the same as for 2016. Thus the same number of samples have been used for the skill scores.

The results indicate that KO performs similarly to CAPE. In this experiment KO leads to higher POD, but due to also lower FAR the CSI is lower as well. However, the differences are relative small. By consideration of the results given in table Table 1 it is obvious that a higher CSI could be gained with KO by decrease of the KO threshold. The combination of KO and CAPE does not lead to better skill scores than KO alone.

The accuracy is close to 100 % for all experiments and is therefore not an appropriate skill score for Cb detection, although, it is sometimes used as score for events with low probability of occurrence.

Table 1. Results of the different experiments. Δ means the difference of IR channels, whereby WV means that of the the water vapor channels, otherwise the channels are explicitely noted. NWP/period provides the model used for NWP filtering and whether the investigated summer period was in 2016 or 2017. IFS is the forecast model of ECMWF and ICON of DWD. The other columns provide the probability of detection (POD), false alarm rate (FAR) and the critical success index (CSI)

Nr	Experiment settings: Cb if	NWP/period	POD(%)	FAR(%)	CSI(%)
1	$\Delta\ BT_{WV} >$ -1 K and CAPE > 60 ore TX > 50	IFS/2016	84.0	20.1	69.4
2	$\Delta\ BT_{WV} > -1K$, without NWP filtering	none/2016	86.3	35.2	58.7
3	$\Delta\ BT_{WV} - 2K$ and CAPE > 60 ore TX > 50	IFS/2016	87.8	26.9	66.4
4	$\Delta\ BT_{WV} > -2K$, without NWP filtering	none/2016	89.9	46.4	50.5
5	$\Delta\ BT_{WV} >$ -1 K and CAPE > 60 ore TX > 50 ore $\Delta\ BT_{IR9.7-IR8.7} > 6K$	IFS/2016	85.5	25.4	66.2
6	$\Delta\ BT_{WV} >$ -1 K and CAPE > 60 ore TX > 50 ore $\Delta\ BT_{IR9.7-IR8.7} > 8K$	IFS/2016	85.5	25.4	66.2
7	$\Delta\ BT_{WV} > -1K$ and CAPE > 45 ore TX > 50	IFS/2016	84.4	22.0	68.1
8	$\Delta\ BT_{WV} > -1K$ and CAPE > 75 ore TX > 50	IFS/2016	83.7	18.9	70.1
9	$BT_{IR10.6} > 224K$ and CAPE > 60 ore TX > 50	IFS/2016	85.2	21.5	69.1
10	$\Delta\ BT_{WV} > -1K$ and CAPE > 60 ore TX > 50	ICON/2016	84.3	19.0	70.3
11	$\Delta\ BT_{WV} > -1K$ and CAPE > 60	ICON/2016	83.5	18.8	70.0
12	$\Delta\ BT_{WV} > -1K$ and CAPE > 60	ICON/2017	87.1	19.0	72.2
13	$\Delta\ BT_{WV} > -1K$ and KO < 3	ICON/2017	89.1	22.8	70.5
14	$\Delta\ BT_{WV} > -1K$ and KO < 3 ore CAPE > 60	ICON/2017	89.2	23.4	70.0

The application of the NWP filter works well independent which of the two NWP models (ICON or ECMWF) or if CAPE ore KO are used as stability filter. One reason for this finding might be that the NWP parameter are applied as filter to filter stable and neutral atmospheres and are therefore very permeable for satellite based Cb detection as soon as labile atmospheric conditions occurs.

4. Discussion

The results of our study show that the 1 channel approach works as good as the established BT difference approach and the investigated 4 channel approach. This might be astonishing on a first glance and the physics behind this finding is therefore briefly discussed.

The radiation signal from optical thick clouds results from the top of the cloud. Thus, concerning Cbs the satellite observes only the top of the cloud. A long history of publications provide evidence that optical thick clouds can be treated as blackbody. This means that the the Stefan Boltzmann law can be applied for radiances emitted by optical thick clouds.

BT defined by the Stefan-Boltzmann law, which results from Planck equation.

$$R = \sigma * T^4 \tag{6}$$

In other words ϵ_λ can be assumed to be 1 in the grey body version of the Stefan-Boltzmann law.

$$R_\lambda = \epsilon_\lambda * \sigma * T^4 \tag{7}$$

This means that in all channels the information of the cloud target (for optical thick clouds) is equal and results simply from the temperature of the cloud top. Thus, there is no possibility to apply IR spectroscopy and additional channels does not provide additional information about the cloud physical properties or if the cold temperature results from a mature (active) Cb or another type of optical thick cloud. Following a brief review of the respective publications.

Stephens [17] compared parameterization schemes with observational data and found that ϵ_λ equals 1 for clouds with a liquid water path (LWP) above a 80-120 (g/m^2). This finding is independent on the cloud type. Beside Cbs, e.g. also cumulus clouds, nimbostratus clouds and stratocumulus II clouds can easily exceed 120 g/m^2 [17]. Further, for the same LWP the emissivity is quite similar for different cloud types below 80-120 (g/m^2), with exception of Stratus II. Please see [18] for a description of the cloud types.

Further, he discussed a parameterization of the effective emissivity of clouds, given in equation 8

$$\epsilon_\lambda = 1 - exp(-a_0 * W) \tag{8}$$

Here a_o is the absorption mass coefficient for total infrared flux (empirically found to be 0.13) and W is the total vertical liquid water path. It is evident that this parameterization leads to an ϵ_λ of 1 for high W. This parameterization is well established and widely used in different fields.

Lio [19] reports that the monochromatic flux emissivity ϵ_λ is given to a good accuracy by

$$\epsilon_\lambda = 1 - exp(-D * a_0(\lambda) * W) \tag{9}$$

This form of the parameterization, with a D=1.66 is aplied as parameterization of ice clouds for climate models [20]. The reader should note that averaging over wavelength is usually necessary in global models for practical reasons. Nevertheless the form remains the same.

Also [21] applied a similar parameterization as [17] for the study of cumulus clouds, but uses the optical depth instead of the LWP path. Equation 8 transforms therefore to

$$\epsilon_\lambda = 1 - exp(-0.75 * \tau_c) \tag{10}$$

here, τ_c is the total cloud optical depth. A similar equation, but with an factor of -0.5 instead of -0.75, is applied for radiance fitting within the scope of Remote Sensing of cloud top pressure/height from SEVIRI [3]. Both, approaches lead to a emissivity of 1 for optically thick clouds.

[22] compared a fast radiative transfer model (RTM) with DISORT [23] and found for the 8.5-,11-,12- μm wavelength that the brightness temperature difference between the models decrease to negligible values with increasing optical depth of ice clouds. This means that optical thick (opaque) ice clouds behave like blackbodies within the uncertainties of the RTMs. This result is in accordance with the above mentioned RTM parameterizations.

[24] uses the blackbody feature of Cbs as basis for the determination of the Effective Emissivity of semitransparent cirrus clouds by bi-spectral measurements based on AVHRR channels 4 and 5 (10.3-11.3 μm and 11,5 - 12,5 μm). [25] uses the same approach for with GMS-1 data.

[26] investigated the long-wave optical properties of water clouds and rain with Mie scattering theory for the wavelength region 5-200 μm. They found that for the long-wave radiation (IR) the cloud becomes a black-body for large LWP (large means greater than 100).

Finally, [27] discussed physics principles in radiometric infrared imaging of clouds in the atmosphere. He investigated also IR emissivity by application of the RTM MODTRAN [28] . His results confirms that the emissivity of optically thick clouds is 1, and that they emit a nearly ideal blackbody spectrum.

Summarizing, clouds with large optical thickness behave as blackbodies in the IR SEVIRI channels. By consideration of the uncertainty of the radiance measurements and calibration uncertainties of the satellite instrument it is evident that IR spectroscopy can not be applied to retrieve information beyond

the temperature of the cloud top for optical thick clouds. Thus, a MSG multiple channel approach does not provide information if the cold cloud is a active Cb or another optical thick cloud. Thus, they can not be used to reduce the FAR of the satellite based detection of Cbs. Contrarily, this can be done by application of the NWP filter as demonstrated in section 3

Using the water vapour brightness temperature difference eases the visible inspection of images and is beneficial for the application of optical flow, applied for the short term forecast of Cbs. However, similar skill scores can be achieved with a 1 channel approach.

Finally, it might be reasonable to clarify why different BT differences occurs (equivalent to different RGB images) if different channels are used, see for example figure 2 in [16]. For the WV channels, as well as for the ozone and CO2 channel the atmospheric signal received by the satellite results from a mixture of the radiation emitted by clouds and from of emission by water vapor, ozone or CO2 for the WV, ozone and CO2 channels, respectively. This interaction leads to different BT signals depending on the chosen channels for the calculation of the BT differences. Thus, this leads to a different relation between the observed brightness temperatures and the cloud top height.

5. Materials and Methods

For the forecast runs ECMWF operational model [12] at 00h and 12h has been used. This means that forecasts up to 9 hours are applied. For comparison ICON [13] has been used. In contrast to ECMWF ICON forecast runs are applied every 3 hours. Thus, the respective run 3 hours prior relative to the satellite scanning time has been used.

The satellite Brightness temperature are derived from the level 1.5 rectified image data of digital counts by application of the Eumetsat calibration coefficients and conversation method. More detailed information on MSG and the SEVIRI instrument are given [29].

The lightning data and the applied methods are discussed in detail in section 3 and section 2, respectively.

6. Conclusions

The performed experiments shows that the satellite based detection of Cbs can be significantly improved by application of an appropriate NWP stability filter. The application of NWP filtering leads to a large decrease of FAR and a large increase of CSI, demonstrating the performance of the filter to separate Cb clouds from other optical thick clouds. The decrease of POD, resulting from the NWP filtering, can be compensated by a reduction of the BT threshold. Thus, NWP filtering can be used to optimize the relation between POD and FAR and to improve the detection scores. Hence, also for applications where a high POD is the primarily goal, and FAR is of second priority, the NWP filter is of vital importance. We show that KO index as well as CAPE are appropriate NWP stability filter. Further more, using ECMWF or ICON forecasts as source for stability filters lead to a similar performance in our experiments. Optical thick clouds behave as black bodies. IR spectroscopy can therefore not be applied in order to decide if a cold optical thick cloud is a active Cb or another cloud type. Thus, a multiple channel approach can not replace the function of NWP filtering. As a result of the study DWD implemented the method based on the brightness temperature difference with a threshold of -1 Kelvin and KO as NWP stability filter as operational Cb detection method for aviation.

Acknowledgments: We thank the weather forecast team of DWD, in particular Mr. Koppert, Mr. Barsleben and Mr. Diehl for the discussion and advice concerning the development of the Cb detection method, in particular concerning the selection of the NWP stability parameters.

Author Contributions: Richard Mueller developed the method and performed the validation study supported by Stephane Haussler. Matthias Jerg initialised and managed the project and contributed to the writing of the manuscript.

Conflicts of Interest: The authors declare no conflict of interest

Abbreviations

The following abbreviations are used in this manuscript:

ACC	Accuracy or hit rate
BT	Brightness Temperature
Cb	Cumulonimbus
CSI	Critical Success Index
CTH	Cloud Top Height
ECMWF	European Centre for Medium Weather forecast.
FAR	False Alarm Rate
ICON	NWP model of Deutscher Wetterdienst
KO	Convection Indec
MSG	Meteosat Second Generation
Meteosat	Meteorological satellite
NWP	Numerical Weather Prediction
POD	Probability of Detection
SEVIRI	Spinning enhanced visible and infrared imager

References

1. Gijben, M.; Coning, C. Using Satellite and Lightning Data to Track Rapidly Developing Thunderstorms in Data Sparse Regions. *Atmospher* **2017**, *8*.
2. Donovan, M.F.; Williams, E.R.; Kessinger, C.; Blackburn, G.; Herzegh, P.H.; Bankert, R.L.; Miller, S.; F., M. The Identification and VErificantion of Hazardous Convective Cells over Oceans Using Visible and Infrared Satellite Observations. *Journal of Applied Meteorology and Climatology* **2008**, *47*.
3. Hamann, U.; Walther, A.; Baum, B.; Bennartz, R.; Bugliaro, L.; Derrien, M.; Francis, P.N.; Heidinger, A.; Joro, S.; Kniffka, A.; Le Gléau, H.; Lockhoff, M.; Lutz, H.J.; Meirink, J.F.; Minnis, P.; Palikonda, R.; Roebeling, R.; Thoss, A.; Platnick, S.; Watts, P.; Wind, G. Remote sensing of cloud top pressure/height from SEVIRI: analysis of ten current retrieval algorithms. *Atmospheric Measurement Techniques* **2014**, *7*, 2839–2867.
4. Mosher, F. Detection of deep convection around the globe. Preprints, 10th Conf. on Aviation, Range, and Aerospace Me- teorology. American Meteorological Society, 2002, pp. 289–292. Portland.
5. Schmetz, J.; Tjemkes, A.; Gube, M.; van der Berg, L. Monitoring deep convection and convective overshooting with Meteosat. *Advances in Space Research* **1997**, *19*, 433–441.
6. Autones, F. Algorithm Theoretical Basis Document for Rapid Development Thunderstorms. Technical report, NWC-SAF, 2013.
7. Tag, P.M.; Bankert, L.R.; Brosy, L.R. An AVHRR multiple cloud-type classification package. *Journal of Applied Meteorology* **2000**, *39*, 125–134.
8. Berendes, T.A.; Mecikalski, J.R.; Mackenzie, W.M.J.; Bedka, K.M.; Nair, U.S. Convective cloud identification and classification in daytime satellite imagery using standard de- viation limited adaptive clustering. *Journal of Geophsical Research* **2008**, *113*.
9. Zinner, T.; Forster, C.; de Coning, E.; Betz, H.D. Validation of the Meteosat storm detection and nowcasting system Cb-TRAM with lightning network data – Europe and South Africa. *Atmospheric Measurements Techniques* **2013**, *6*, 1567–1583.
10. Moncrief, M.W.; Miller, M.J. The dynamics and simulation of tropical cumulonimbus and squall lines. *Q. J. R. Meteorol. Soc.* **1976**, *120*, 373–394.
11. www.ecmwf.int/en/forecasts/documentation-and-support/changes-ecmwf-model/ifs-documentation. last visit 10.09.2017.
12. Bechtold, P.; Köhler, M.; Jung, T.; Doblas-Reyes, F.; Leutbecher, M.; Rodwell, M.J.; Vitart, F.; Balsamo, G. Advances in simulating atmospheric variability with the ECMWF model: From synoptic to decadal time-scales. *Quarterly Journal of the Royal Meteorological Society* **2008**, *134*, 1337–1351.
13. Zängl, G.; Reinert, D.; Rípodas, P.; Baldauf, M. The ICON (ICOsahedral Non-hydrostatic) modelling framework of DWD and MPI-M: Description of the non-hydrostatic dynamical core. *Quarterly Journal of the Royal Meteorological Society* **2015**, *141*, 563–579.

14. Betz, H.D.; Schmidt, K.; Laroche, P.; Blanchet, P.; Oettinger, W.P.; Defer, E.; Dziewit, Z.; Konarski, J. LINET — An international lightning detection network in Europe. *Atmospheric Research* **2009**, *91*, 564 – 573.
15. Betz, H.; Schmidt, K.; Oettinger, W.; Montag, B. Cell-tracking with lightning data from LINET. *Advances in Geoscience* **2008**, *17*, 55–61.
16. Mikuš, P.; Mahović, N.S. Satellite-based overshooting top detection methods and an analysis of correlated weather conditions. *Atmospheric Research* **2013**, *123*, 268–280.
17. Stephens, G. Radiation Profiles in Extended Water Clouds II: Parameterization Schemes. *J. Atmos. Sci.* **1978**, *35*, 2123–2132.
18. Stephens, G. Radiation Profiles in Extended Water Clouds I: Theory. *J. Atmos. Sci.* **1978**, *35*, 2111–2122.
19. Liou, K. *Radiation and cloud processes in the atmosphere*; Oxford University Press, 1992.
20. Ebert, E.E.; Curry, J.A. A Parameterization of Ice Cloud Optical Properties for Climate Models. *Journal of Geophysical Research* **1992**, *97*, 3831–3836.
21. Xu, K.M.; Randall, D.A. Impcat of Interactive Radiative Transfer on the Macroscopic Behaviour of Cumulus Ensembles. Part I: Radiation Parameterization and Sensitivity Tests. *Journal of the Atmospheric Sciences* **1995**, *52*, 785–799.
22. Wang, C.; Yang, P.; Baum, B.A.; Platnick, S.; Heidinger, A.K.; Hu, Y.; Holz, R.E. Retrieval of Ice Cloud Optical Thickness and Effective Particle Size Using a Fast Infrared Radiative Transfer Model. *Journal of Applied Meteorology and Climatology* **2011**, *50*, 2283–2297.
23. Spurr, R.; Kurosu, T. A Linearized Discrete Ordinate Radiative Transfer Model for Atmospheric Remote Sensing Retrieval. *J. Quant. Spec. Radiat. Trans.* **2001**, *68*, 689–735.
24. Inoue, T. On the Temperature and Effective Emissivity Determination of Semi-Transparent Cirrus Clouds by Bi-Spectral Measurements in the 10 μm window region. *Journal of the Meteorological Society of Japan* **1985**, *63*, 88–99.
25. Nasuda, H. Infrared Greybody Emissivity and Visible Albedo of High Altitude Semitransparent Cloud. *?* **1985**.
26. Savijäri, H.; Räisänen, P. Long-wave optical properties of water clouds and rain. *Tellus* **1998**, *50A*, 1–11.
27. Shaw, J.A.; Nugent, P.W. Physics principles in radiometric infrared imaging of clouds in the atmosphere. *European Journal of Physics* **2013**, *34*.
28. Abreu, L.; Anderson, G. The MODTRAN 2/3 Report and LOWTRAN 7 MODEL. Technical report, Philips Laboratory, Hanscom, 1996.
29. Schmetz, J.; Pili, Tjemkes, P.S.; Just, D.; Kerkmann, J.; Rota, S.; Ratier, A. An introduction to Meteosat Second Generation (MSG). *Bull. Am. Met. Soc.* **2002**, pp. 977–992.